We are IntechOpen,
the world's leading publisher of
Open Access books
Built by scientists, for scientists

4,800
Open access books available

122,000
International authors and editors

135M
Downloads

Our authors are among the

154
Countries delivered to

TOP 1%
most cited scientists

12.2%
Contributors from top 500 universities

CLARIVATE ANALYTICS
BOOK CITATION INDEX
INDEXED

WEB OF SCIENCE™

Selection of our books indexed in the Book Citation Index
in Web of Science™ Core Collection (BKCI)

Interested in publishing with us?
Contact book.department@intechopen.com

Chapter

Topics of Analytical and Computational Methods in Tunnel Engineering

Michael G. Sakellariou

Abstract

In this chapter, a selection of tunneling topics is presented, following the evolution of methods and tools from analytical to computational era. After an introductory discussion of the importance of elasticity and plasticity in tunneling, some practical topics are presented as paradigms to show the successful application of them in achieving a solution. The circular and horseshoe tunnel sections served as the basis of the elastic analysis of deep tunnels. Practical aspects such as influence zone and elastic convergences in both cases are examined. In the case of circular tunnels, the estimation of plastic zone formation is discussed for a selection of strength criteria. After a detailed discussion of the influence of surface proximity, the elastic and plastic analysis of shallow tunnels is examined in some detail. The presentation is completed by a short presentation of computational methods. An overview of recent developments and a classification of the methods are presented, and then some problems for the case of anisotropic rocks have been presented using finite element method (FEM). The last topic is the application of artificial intelligence (AI) tools in interpreting data and in estimating the relative importance of parameters involved in the problem of tunneling-induced surface settlements. In the conclusions a short discussion of the main topics presented follows.

Keywords: elasticity, plasticity, deep tunnels, shallow tunnels, influence zone, plastic zone, circular tunnels, horseshoe tunnels, computational methods, ANN, surface settlements

1. Introduction

Underground work history goes back to prehistoric times [1]. The oldest known tunnel is the one underpassing the River Euphrates in Babylon constructed 4000 years ago. Hezekiah, King of Judea, built a tunnel 2700 years ago, whereas Eupalinos built the Eupalinion tunnel constructed in Samos Island, Greece, 2600 years ago, both for water supply purposes. For further information see [2–5]. Shelters, underground works for warfare purposes, mineral resource exploitation, traffic tunnels and conveyance tunnels like water supply tunnels, etc. are the main categories of underground structures [3].

Tunnel engineering could be characterized as an art, not fine art of course, with the meaning of know-how based on past experience, lessons learned from tunnel disasters [6], knowledge of geological conditions and behaviour of the ground,

innovations to overcome encountered difficulties, scientific knowledge from applied mechanics and advances in mechanized excavation tools and methods. In recent years, the experience from South Africa and North Europe rock engineering practice resulted in the introduction of comprehensive classification systems, namely, RMR [7, 8] and Q system [9]. In theory, Lamé in 1852 and Kirsch in 1898 [10] paved the road of scientific development of solutions to the problem of stresses and strains around underground holes [10]. Terzaghi [11] examined shallow tunneling through sands and cohesive soils. For a comprehensive presentation of the fundamentals of theoretical rock mechanics, see Jaeger et al. [12]. For a detailed coverage of underground excavations in rock, see Hoek and Brown [13]. Experimental methods such as photoelasticity [14, 15] and Moiré [16] and computational methods such as finite elements [17], finite difference, direct and indirect boundary elements [13, 18], distinct elements [19] and meshfree methods [20, 21] have been developed and extensively applied successfully. On the other hand, the progress regarding the material behaviour resulted in advanced constitutive laws [22] and in the more realistic modeling of continua and discontinua media [23]. Finally, the information systems and in particular the artificial intelligence offered new tools like artificial neural networks (ANN) and other machine learning methods.

2. Analytical methods: elastic problems

2.1 The case of deep tunnels

Deep tunnels can be considered as the limiting case of a cylinder with thick walls when the radius of the exterior wall tends to infinity. In that case the ground surface has no any influence on the stress field around the opening.

Jeffery [24] solved the problem of stress distribution inside the walls of a cylinder bounded by two non-concentric circles, with the distance of their centres denoted by d. In this way, Jeffery's approach solves the problems of an infinite plate containing a circular hole as the limit of a thick cylinder with concentric boundaries (d = 0) and the problem of a semi-infinite plate containing a circular hole as a particular case of two eccentric boundaries. So, he gave the general solution of deep and shallow tunnels, respectively, as particular cases of a general problem.

For a historical account of the mathematical solutions of stress distribution around underground openings, see Gerçek [25].

2.1.1 Cyclic section

Assuming a homogeneous isotropic linear elastic medium (HILE medium) and considering the geometry of the problem and the equations of equilibrium, we obtain the following set of equations (Eqs. (1)–(4)) (**Figure 1**):

$$\sigma_r = -\frac{2G}{1-2\nu}\left\{\frac{A}{2} - (1-2\nu)\frac{B}{r^2}\right\}, \Rightarrow \sigma_r = C - \frac{D}{r^2}, \tag{1}$$

$$\sigma_\theta = -\frac{2G}{1-2\nu}\left\{\frac{A}{2} + (1-2\nu)\frac{B}{r^2}\right\}, \Rightarrow \sigma_\theta = C + \frac{D}{r^2}, \tag{2}$$

$$\tau_{r\theta} = 0 \tag{3}$$

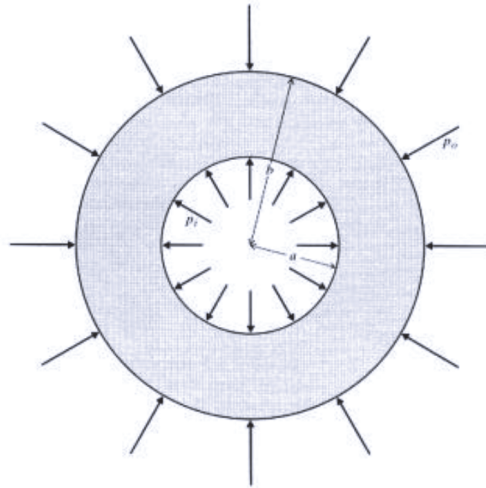$$u_r = -\frac{1}{2G}\left\{(1-2\nu)Cr + \frac{D}{r}\right\} \tag{4}$$

Figure 1.
The cylinder with thick walls.

The constants C and D are defined as:

$$C = -\frac{GA}{1 - 2\nu},$$
$$D = -2GB$$

Considering the boundary conditions:
for $r = a$, $\sigma_r = p_a$.
$r = b$, $\sigma_r = p_b$.

therefore:

$$p_a = C - \frac{D}{a^2},$$
$$p_b = C - \frac{D}{b^2}$$
$$D = \frac{(p_b - p_a)a^2 b^2}{(b^2 - a^2)},$$
$$C = \frac{(b^2 p_b - a^2 p_a)}{(b^2 - a^2)}$$

When b tends to infinity, we obtain the special case of a cyclic opening excavated in an infinite medium under hydrostatic stress field p, by superposing the initial stresses induced by the excavation:

$$\sigma_r = p\left(1 - \frac{a^2}{r^2}\right),$$
$$\sigma_\theta = p\left(1 + \frac{a^2}{r^2}\right),$$
$$\tau_{r\theta} = 0,$$
$$u_r = -\frac{1}{2G}\frac{a^2}{r}p$$

(5)

For the general case of stress field, denoting the ratio of horizontal to vertical in situ principal stress with k, Kirsch [10] obtained the following equations:

$$\sigma_r = \frac{p}{2}\left[(1+k)\left(1-\frac{a^2}{r^2}\right)-(1-k)\left(1-4\cdot\frac{a^2}{r^2}+3\cdot\frac{a^4}{r^4}\right)\cos 2\theta\right],$$

$$\sigma_\theta = \frac{p}{2}\left[(1+k)\left(1+\frac{a^2}{r^2}\right)+(1-k)\left(1+3\cdot\frac{a^4}{r^4}\right)\cos 2\theta\right],$$

$$\tau_{r\theta} = \frac{p}{2}\left[(1-k)\left(1+2\cdot\frac{a^2}{r^2}-3\cdot\frac{a^4}{r^4}\right)\sin 2\theta\right], \qquad (6)$$

$$u_r = -\frac{pa^2}{4Gr}\left[(1+k)-(1-k)\left\{4(1-v)+\frac{a^2}{r^2}\right\}\cos 2\theta\right],$$

$$u_\theta = -\frac{pa^2}{4Gr}\left[(1-k)\left\{2(1-2v)+\frac{a^2}{r^2}\right\}\sin 2\theta\right],$$

It is interesting to note that in the case of hydrostatic or isotropic stress field (k = 1), we can estimate an influence zone accepting a ± 0.04% deviation from the initial stress field. Then by introducing this condition in the above equations, we obtain the radius of influence zone as 5α, where α is the radius of the excavation.

2.1.2 The case of horseshoe section

Let us examine now the case of horseshoe section (**Figures 2** and **3**). This problem is very useful in the case of excavations without using a tunnel boring machine (TBM). **Figure 2** shows a typical metro section, whereas **Figure 3** shows the simplified section used in the analysis.

First, the maximum principal stress σ_1 contours obtained by a numerical analysis are shown **Figure 4**. A slight influence of the asymmetric shape of the tunnel's section can be observed. Schürch and Anagnostou [26] examined the influence of rotational symmetry violation on the applicability of the ground response curve.

To obtain a solution to this problem, we adopted Muskhelishvili approach, using functions of complex variables and conformal mapping techniques [27].
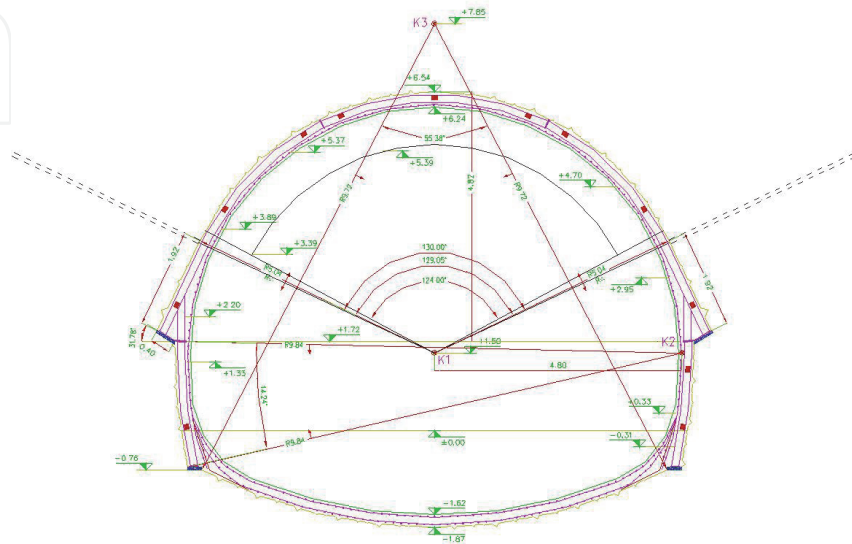

Figure 2.
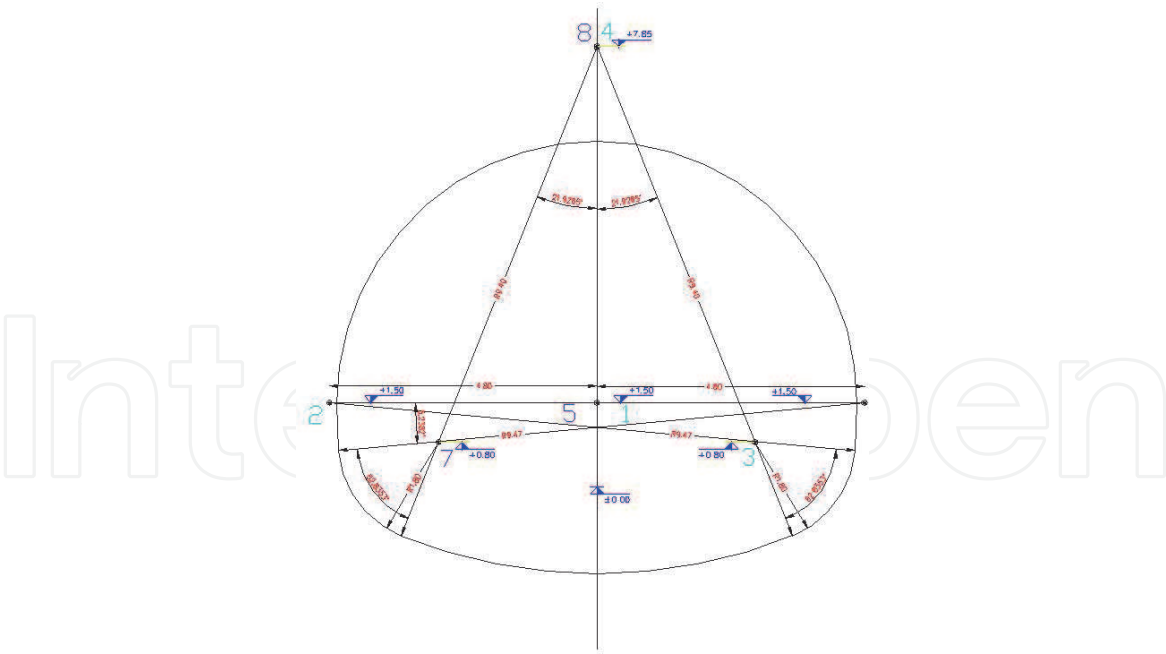*Typical horseshoe tunnel section.*

Figure 3.
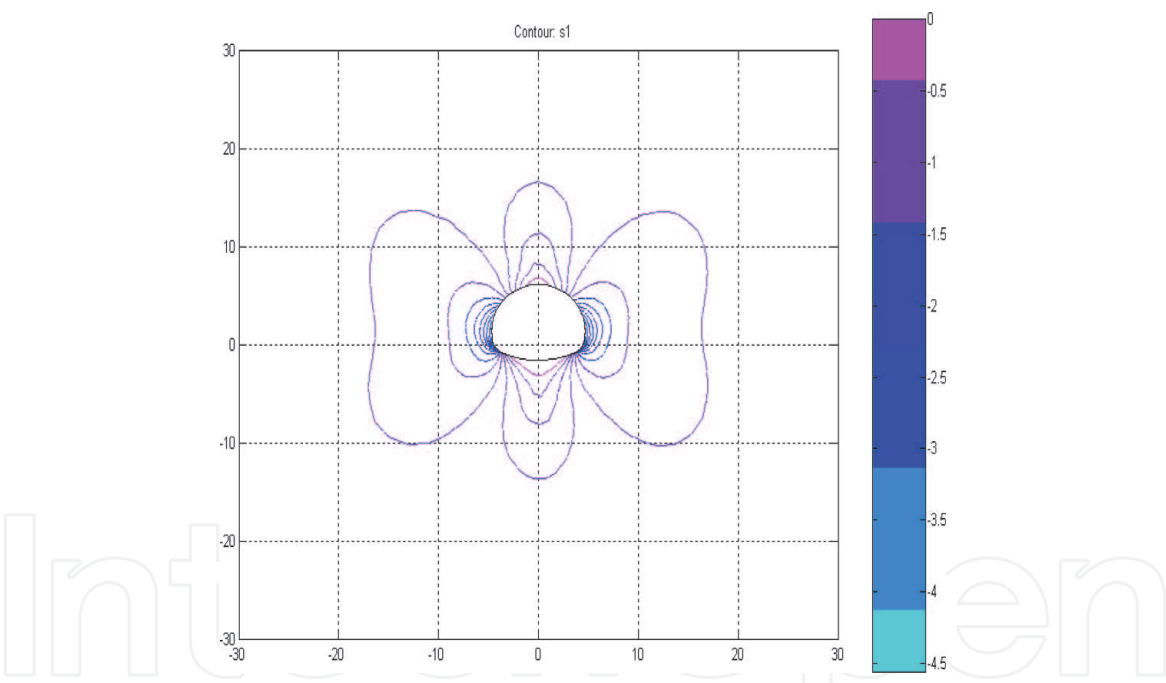*A simplified horseshoe tunnel section.*

Figure 4.
Maximum principal stress contours around a deep horseshoe tunnel section.

Adopting Gerçek solution [28], we introduce the following mapping function, which transforms the infinite region surrounding the opening onto the interior of the unit circle (**Figure 5**):

$$z = \omega(\zeta) = R\left(\frac{1}{\zeta} + \sum_{k=1}^{3} a_k \cdot \zeta^k\right) \tag{7}$$

In Eq. (7) R is a real constant, and the complex coefficients α_k are defined as:

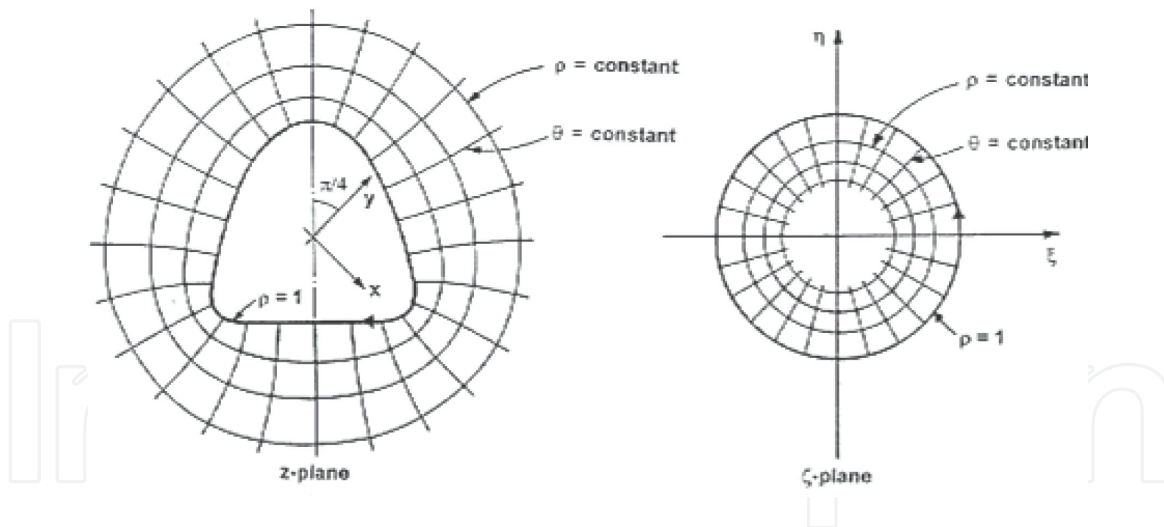$$a_k = \alpha_k + b_k, \text{ for } k = 1,2,3 \tag{8}$$

Figure 5.
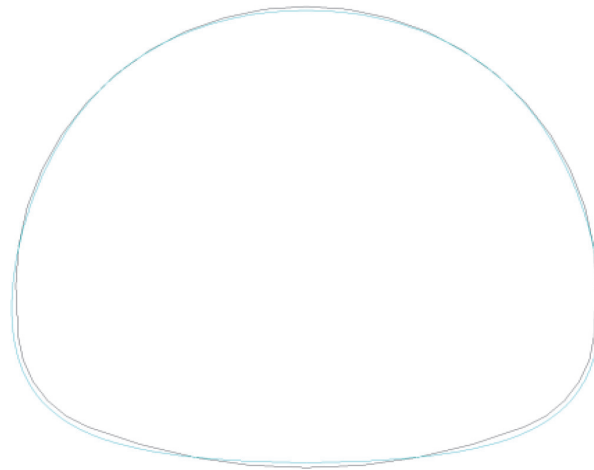*Conformal mapping of an infinite region surrounding a hole onto the unit circle [28].*

Figure 6.
The final section that best fits the initial horseshoe section [29, 30].

In order to find the optimum values of the above coefficients to fit best the given *horseshoe section, a (123x3) system of equations has been solved* [29, 30]. *The values of the coefficients are:*

$$\alpha_1 = b_3 = 0$$
$$\alpha_2 = b_2 = 0.047,$$
$$\alpha_3 = 0.029,$$
$$b_1 = 0.104,$$
$$R = 3.756$$

(9)

In [29, 30] an extended investigation of this problem is presented resulting in the calculation of the set of coefficients for 49 sections. In **Figure 6**, the final section, which is the best for our problem, is presented superimposed to the original horseshoe shape.

Now, we can calculate the stresses around the opening as well as the strains for initial stress fields with k = 0, 0.333, 1 and 3 [29, 30]. In **Figures 7** and **8**, the variation of σ_θ at the boundary of the excavation is shown for k = 0.333 (**Figure 7**) and k = 1 (**Figure 8**).
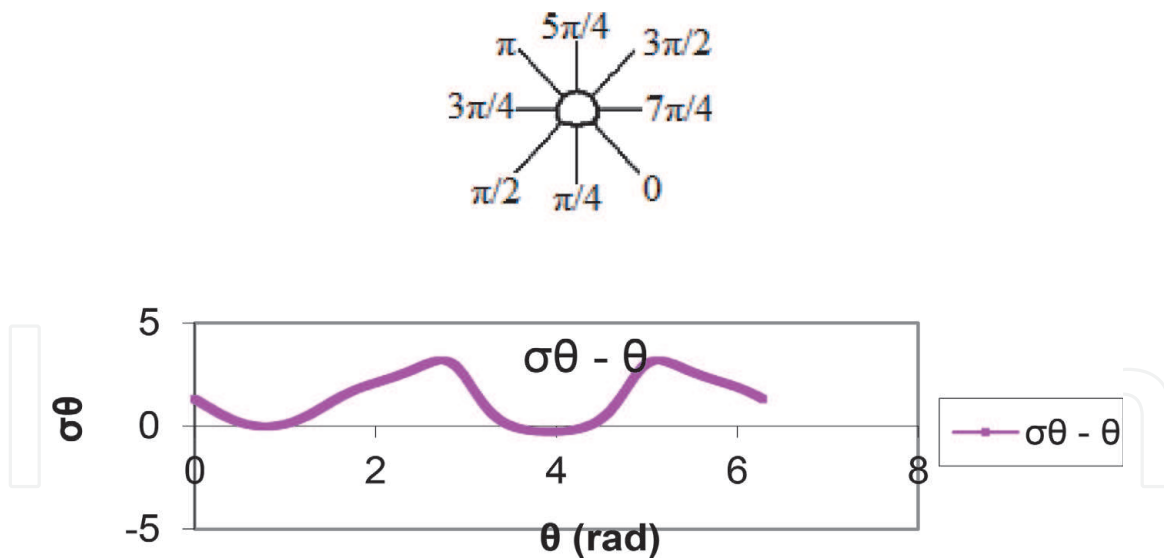
Figure 7.
Hoop stress σ_θ variation along the boundary of the excavation for k = 0.333 [29].
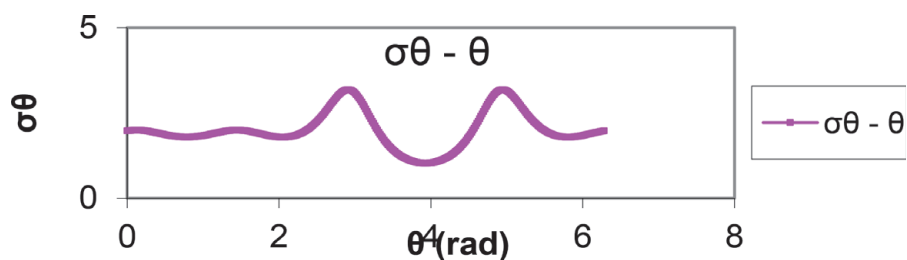

Figure 8.
Hoop stress σ_θ variation along the boundary of the excavation for k = 1 [30].

Initial stress field	Convergences of circular section [mm]	Horseshoe-induced roof convergences [mm]	Horseshoe-induced bottom convergences [mm]
k = 1	7.8	7.6	8.2
k = 0.333	7.1	7.0	7.9
k = 1	5.6	5.9	7.2
k = 3	1.1	2.5	5.0

Table 1.
Convergences of circular and horseshoe sections for different stress fields [29, 30].

A further result of practical significance obtained by this method is the calculation of the convergence of the excavation boundaries and the extent of the zone of influence. In **Tables 1** and **2**, these values are presented in comparison with the corresponding values for the circular section. We can observe the greater deviation at the bottom of the horseshoe section because of the greater radius of this segment compared to the circle.

In all cases presented in this paragraph, we assumed the initial stress field p = 1 MPa, modulus of elasticity E = 1 GPa and Poisson ratio ν = 0.3. Using these values we are able to calculate the corresponding values for any p value and every kind of rock. The only constraint is that the value of Poisson ratio is equal to 0.3. In the following paragraph, we shall discuss the influence of ν upon the stresses.

Initial stress field	Influence zone (horseshoe section)	Influence zone (circular section)
k = 0	8.6R	7.5R
k = 0.333	7.8R	7R
k = 1	5.6R	5R
k = 3	7.4R	7R

R is the radius of equivalent circular section [29, 30].

Table 2.
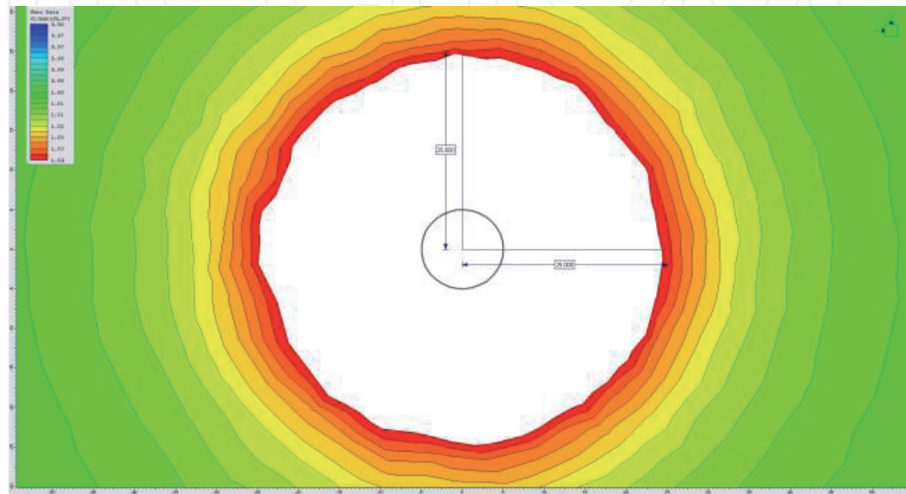*Influence zone extends around circular and horseshoe sections for different stress fields.*

Figure 9.
Stress distribution around a circular deep tunnel (Z = 25R, k = 1) [32].

2.2 The case of shallow tunnels: the circular section

Assuming that the tunnel is close to the ground surface, we can observe an influence of the boundary as the vertical stresses depend on the depth. So, the initial stresses at the roof and the bottom levels of the tunnel section are not equal. Bray [31] presented an extensive study on this problem. Some practical rules are summarized below.

By assuming an acceptable deviation, as in the case of the influence zone estimation, we may distinct three cases.

2.2.1 Case I

The tunnel depth, measured from the section's centre, is Z > 25R, where R is the tunnel radius. In this case Kirsch equations apply. In **Figure 9**, the distribution of stresses around a circular deep tunnel is shown [32]. There is no influence of the boundaries. Note that only a window of the stress field is shown.

2.2.2 Case II

The tunnel depth is 7R < Z < 25R. In this case we must add a correction term to the Kirsch equations depending on the Poisson ratio. That term is given by Bray as [31]:

$$\sigma_\theta = \gamma h[1 + k + 2(1-k)\cos 2\theta] - \gamma\alpha\sin\theta\left[\frac{3-4\nu}{2(1-\nu)} + 2(1-k)\cos 2\theta\right] \qquad (10)$$
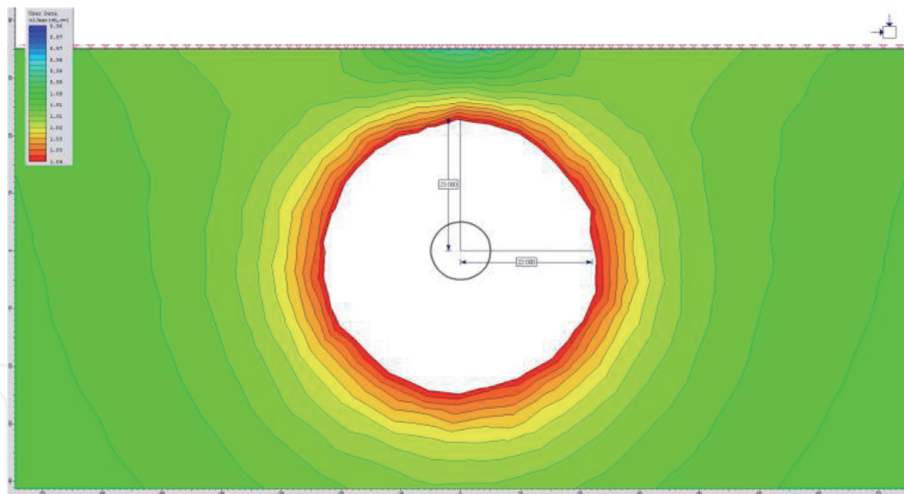
Figure 10.
Stress distribution around a circular shallow tunnel (Z = 7R, k = 1) [32].

where α is the tunnel's radius. This expression agrees with an equation given by Savin [33].

In **Figure 10**, the distribution of stresses around a circular shallow tunnel is shown. The influence of the surface boundary starts to be noticeable [32].

2.2.3 Case III

The tunnel depth is Z < 7R. This case is more difficult because the influence of the boundary becomes greater. Then Mindlin's closed-form solutions apply [34, 35]. Mindlin obtained solutions to this problem for three cases of in situ stress fields at depth z (remote from the tunnel):

2.2.3.1 Case I

p_z = wz.
p_h = wz.

i.e. isotropic, or hydrostatic, gravitational pressure and w being the unit weight of mass.

2.2.3.2 Case II

p_z = wz.
p_h = {$\nu/(1-\nu)$}wz.

This is the case where the lateral deformation is a constraint remote from the tunnel.

2.2.3.3 Case III

p_z = wz.
p_h = 0.

This is the case of nonlateral constraint of the mass remote from the tunnel.

The solutions of Mindlin were in terms of bipolar coordinates α and β. The expression giving the stress on the circular boundary for the first case is [35]:

$$
[\sigma_\beta]_{\alpha=\alpha_1} = \frac{2w\mathrm{A}(\cosh\alpha_1 - \cos\beta)}{\sinh\alpha_1} \left\{ \frac{1 - \cosh\alpha_1\cos\beta}{(\cosh\alpha_1 - \cos\beta)^2} \right.
$$
$$
\left. -\coth\alpha_1 - \frac{(7-8\nu)}{4(1-\nu)}\frac{\cos\beta}{\sinh\alpha_1} + 2e^{-\alpha_1}\cos\beta\sum_{n=2}^{\infty} R_n\cos n\beta \right\} \tag{11}
$$

where α_1 is the value of α corresponding to the boundary of the tunnel:

$$
\frac{Z}{R} = \cosh\alpha_1
$$
$$
A = Z\tanh\alpha_1 = R\sinh\alpha_1
$$
$$
R_n = N_n - ne^{-n\alpha_1} \tag{12}
$$
$$
N_n = \frac{ne^{-n\alpha_1}(\sinh n\alpha_1\cosh n\alpha_1 - n\sinh\alpha_1\cosh\alpha_1)}{\sinh^2 n\alpha_1 - n^2\sinh^2\alpha_1}
$$

Poulos and Davis [35] gave in figures and tables values of σ_β for $1 < (Z/R) < 4$.

For Cases II and III above, the solution for σ_β is obtained by adding in the solution given by Eq. (11) a further expression [33]. From the above analysis, the importance of taking into account the influence of the ground surface on the stress distribution on tunnel boundary is obvious. A further important notice is the influence of Poisson ratio on the expressions of stresses. From Eq. (10), it is clear that this influence is important when $Z < 25R$.

Malvern [36] in a rigorous analysis concluded that when the resultant force on each boundary is zero, then the stress distribution is independent of the elastic constants. Otherwise the stress distribution will depend on ν. When the boundary conditions include displacement constraints, then the stress distribution will, also, depend on ν. These conclusions are important to be known for the stress analysis of tunnels by using computational methods like finite elements or boundary elements. Frocht [14] examined the influence of stresses from ν by extensive photoelastic experimental study. In this short presentation of the elastic solutions for the shallow circular tunnel, we restricted to the stress field influence. For an extensive presentation of elastic solutions for the important problem of surface settlements induced by tunneling, which is of great practical significance, see [37–39]. Another important topic in the case of shallow tunnels is the problem of stress field due to seismic loading. Recently, Pelli and Sofianos [40] published a paper addressing the very important topic of the stress field around shallow tunnels under seismic loading of SW waves.

3. Analytical methods: plastic problems

3.1 The case of deep tunnels

We now turn our interest in plastic problems. This is a case of great theoretical and practical significance, as every underground excavation must be analysed against failure. For a detailed coverage, see, almost, every standard textbook of soil and rock mechanics. For a more detailed coverage, see [41–44]. Here, we examine

special topics related to tunnel engineering. In order to analyse the competence of an excavation in soil or rock, we must extend our analysis beyond elasticity to the plastic behaviour of the surrounding medium. To this end, we have to introduce to our analysis a failure criterion. The most common criterion is the Mohr-Coulomb [11]. Extensive research resulted in a remarkable advancement in understanding the material behaviour and the implementation of advanced models in computational methods. A milestone was the introduction of critical state theory in the 1960s [45]. Further research in rock mechanics resulted in the introduction of the Hoek-Brown criterion, which is widely used in rock engineering practice [13]. Yu [46], in an extensive review, presented a wide range of failure criteria applicable on, almost, every kind of materials under every possible type of loading. In this review Yu discussed as well the soil and rock materials.

Let us examine the problem of practical significance of the formation of plastic zone around a deep tunnel of circular section. Closed-form solutions can be found for every criterion of soil and rock literature in the case of isotropic or hydrostatic stress field (k = 1), because of the axisymmetric type of this case. Recently, Vrakas and Anagnostou presented an extension of the small strain analyzes to obtain finite strain solutions [47]. For the general case of stress fields (k ≠ 1), closed-form solutions have been obtained so far for the Tresca criterion [48] and for the Mohr-Coulomb criterion [49]. Here, the elliptic paraboloid criterion developed by Theocaris [50, 51] is introduced to solve the problem of plastic zone around a circular deep tunnel in rock. First, the mathematical expression of the criterion is given, and a comparison of it with Griffith and Hoek-Brown criteria is presented.

This criterion is expressed through the three principal stresses. It is an energy criterion having as parameter the absolute value of the ratio R of uniaxial compressive strength over the uniaxial tensile strength. The elliptic paraboloid criterion is developed for applications in applied mechanics in general, so the tensile stresses are positive, and the compressive stresses are negative. Then:

$$(\sigma_1 - \sigma_2)^2 + (\sigma_2 - \sigma_3)^2 + (\sigma_3 - \sigma_1)^2 + 2(R-1)(\sigma_1 + \sigma_2 + \sigma_3)\,\sigma_t = 2\,R\,\sigma_t^2 \quad (13)$$

where $R = \dfrac{|\sigma_c|}{\sigma_{t.}}$.

Eq. (13) is the addition of two components, which express two parts of the total elastic energy. Indeed, the first part is, up to a constant multiplicative factor, the distortion energy expressed through the deviatoric stresses. This part represents the energy of the elastic change of shape [52] given by Eq. (14):

$$(\sigma_1 - \sigma_2)^2 + (\sigma_2 - \sigma_3)^2 + (\sigma_3 - \sigma_1)^2 \quad (14)$$

The second part depends on the hydrostatic or spherical part of the stresses and represents the energy of elastic change in volume. In this way, the elliptic paraboloid criterion combines both the change of shape and volume. The latter is important for soil and rock materials as their strength depends on the confining pressure.

For the isotropic case of field stress, conditions of axisymmetry are valid, i.e. $\sigma_1 = \sigma_2$. Then from Eq. (13), we obtain:

$$(\sigma_3 - \sigma_1)^2 + \frac{R-1}{R}(2\sigma_1 + \sigma_3)\sigma_c - \frac{\sigma_c^2}{R} = 0 \quad (15)$$

In the case of axisymmetric conditions, the criterion becomes paraboloid of revolution. In **Figure 11**, a comparison of Griffith criterion with Hoek-Brown criterion being shown. It is obvious that the deviation between their representation
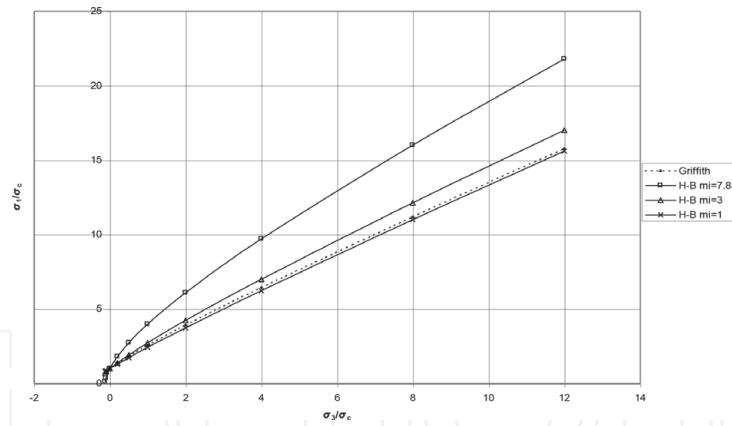
Figure 11.
Comparison of Griffith criterion with Hoek-Brown criterion for different m values [52].

for m value being equal to 7.88, close to the restriction of Griffith's corresponding value being 8 [52].

Now, we can proceed to a comparison of elliptic paraboloid criterion with Griffith. We assume an R value of 8 (**Figure 12**).

From the above figures, we may conclude that Griffith and elliptic paraboloid criteria agree, although their assumptions are completely different. Griffith assumed that failure initiates from pre-existed cracks because of the stress concentration at the tips of the cracks. This assumption is fundamental in fracture mechanics. On the other hand, the assumption of elliptic paraboloid criterion is an extension of von Mises criterion. Both criteria are identical in the case of equal strengths under compression and tension (R = 1). This assumption is close to the experimental results for metals. Theocaris applied this criterion in igneous and metamorphic rocks [45].

We, now, come to examine the problem of plastic zone formation around a deep tunnel of circular section under isotropic stress field (k = 1) [53] (**Figure 13**).

To solve the problem, we introduce the equation of equilibrium in polar coordinates (Eq. (16)) and the flow rule (Eq. (17)). Then, by introducing the expression of elliptic paraboloid criterion in Eq. (17), we obtain Eq. (18) [53]:

$$\frac{d\sigma_r}{dr} + \frac{\sigma_r - \sigma_\theta}{r} = 0 \tag{16}$$

$$\frac{\partial f}{\partial \sigma_2} = 0 \tag{17}$$

$$\frac{\partial\left[(\sigma_1 - \sigma_2)^2 + (\sigma_2 - \sigma_3)^2 + (\sigma_3 - \sigma_1)^2 + 2 \cdot (R_b - 1) \cdot (\sigma_1 + \sigma_2 + \sigma_3) \cdot \sigma_{tb} - 2 \cdot R_b \cdot \sigma_{tb}^2\right]}{\partial \sigma_2} = 0 \tag{18}$$

After complicated algebraic manipulations, we obtain the condition for plastic zone formation around the tunnel (Eq. (19)) [53]:

$$p_o < \frac{(R_i - 1) \cdot \sigma_{ti}}{2} - p_i - \sqrt{-(R_i - 1) \cdot \sigma_{ti} \cdot p_i + \frac{1}{3} \cdot R_i \cdot \sigma_{ti}^2 + \frac{(R_i - 1)^2 \cdot \sigma_{ti}^2}{3}} \tag{19}$$

Finally, the radius of the plastic zone r_c is obtained (Eq. (20)) [53]:

$$r_e = r_i \cdot e^{\frac{L-K}{2 \cdot (R_b - 1) \cdot \sigma_{tb}} - \frac{1}{2} \cdot \ln \frac{K}{L}} \tag{20}$$

L and K above are constants given by Eq. (21), (22):

$$K = -(R_b - 1) \cdot \sigma_{tb} - \sqrt{\frac{4}{3} \cdot R_b \cdot \sigma_{tb}^2 - 4 \cdot (R_b - 1) \cdot \sigma_{tb} \cdot \sigma_{re} + \frac{4 \cdot (R_b - 1)^2 \cdot \sigma_{tb}^2}{3}}$$

(21)

$$L = -(R_b - 1) \cdot \sigma_{tb} - \sqrt{\frac{4}{3} \cdot R_b \cdot \sigma_{tb}^2 - 4 \cdot (R_b - 1) \cdot \sigma_{tb} \cdot p_i + \frac{4 \cdot (R_b - 1)^2 \cdot \sigma_{tb}^2}{3}}$$
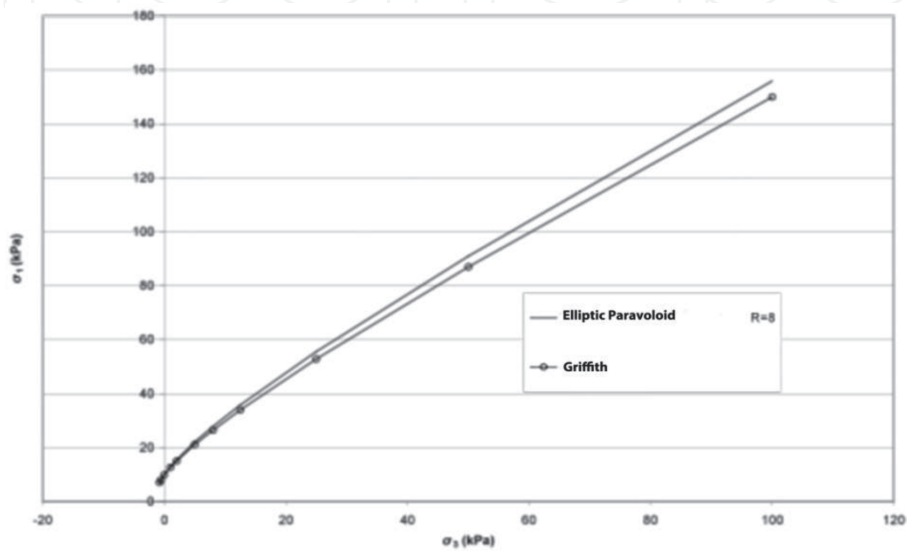
(22)

Figure 12.
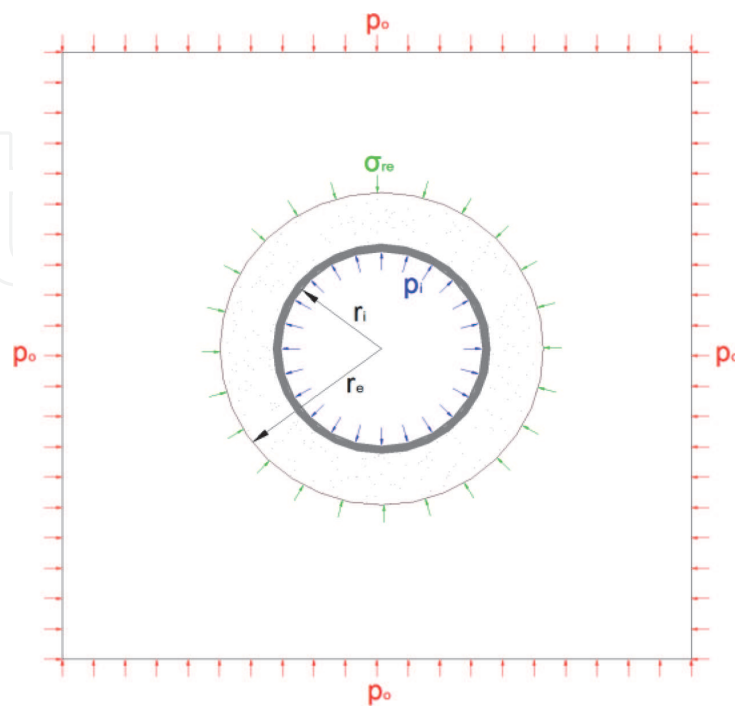*Comparison of elliptic paraboloid and Griffith criteria (R = 8) [52].*

Figure 13.
The geometry of the problem. The plastic zone around the circular tunnel is shown [53].

Hoek and Brown [9] obtained the radius of the plastic zone for Hoek-Brown criterion as follows [13]:

$$r_e = r_i e^{\left\{ N - \frac{2}{m_r \sigma_c} \left(m_r \sigma_c p_i + s_r \sigma_c^2 \right)^{\frac{1}{2}} \right\}} \tag{23}$$

$$N = \frac{2}{m_r \sigma_c} \left(m_r \sigma_c p_0 + s_r \sigma_c^2 - m_r \sigma_c^2 M \right) \tag{24}$$

$$M = \frac{1}{2} \left(\left(\frac{m}{4} \right)^2 + m \frac{p_0}{\sigma_c} + s \right)^{\frac{1}{2}} - \frac{m}{8} \tag{25}$$

In **Table 3** a comparison of the above criteria is shown. We can conclude that, except for low values of in situ stresses, both criteria are close in their predictions of radial stresses at the elastic–plastic interface. On the contrary, their predictions regarding the extent of the plastic zone differ with Hoek-Brown criterion being somehow more conservative.

3.2 The shallow tunnel case

The shallow tunnel case is complicated because of the influence of the proximity of ground surface on the stress field and the influence of gravity. As we notice for the case of deep tunnels, there are closed-form solutions for the plastic zone formation around circular tunnels for isotropic stress field and for the general case of Tresca [48] and Mohr-Coulomb [49] criteria. For the case of shallow tunnels, there were no closed-form solutions until 2009 when a solution was published for the Mohr-Coulomb solution under the assumption of isotropic stress field (k = 1) and no gravitational stresses, based on bipolar coordinates (**Figure 14**).

	Elliptic paraboloid		Hoek-Brown	
P0 (MPa)	σ_{re} (MPa)	r_e (m)	σ_{re} (MPa)	r_e (m)
4	2.10	10.25	1.96	13.45
3	1.35	8.29	1.31	11.22
2	0.64	6.55	0.71	9.07
1.5	0.31	5.76	0.44	7.99
1	0.01	5.02	0.20	6.84

Table 3.
Comparison of elliptic paraboloid and Hoek-Brown criteria for σ_c = 1 MPa, σ_t = 0.125 MPa, R = 8.00, m = 8 and s = 1 [53].
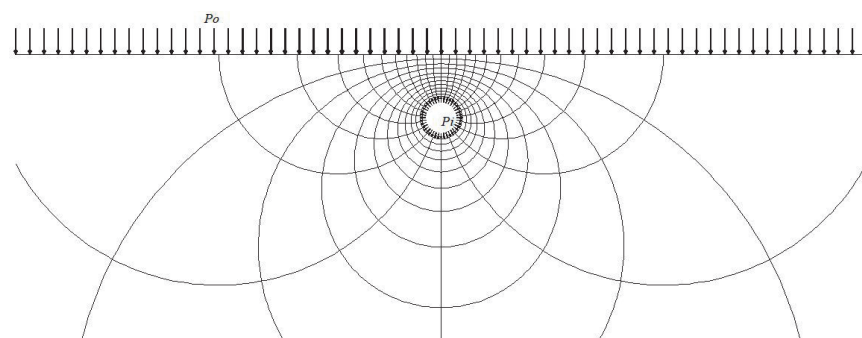

Figure 14.
Bipolar coordinates used for the solution of shallow tunnel problem [54].

In the following the solution published in [54] and further applied [55] is presented omitting the detailed mathematical analysis:

$$
\begin{aligned}
P_{cr} &= \frac{2\kappa^2}{2\left(d_i^2 - r_i^2 \cos^2\beta\right) + \kappa^2(\lambda - 1)}\left[P_0\left(\frac{d_i^2 - r_i^2 \cos^2\beta}{\kappa^2}\right) - \frac{Y}{2}\right] \\
&= \frac{2\kappa^2}{2\left(\kappa^2 + r_i^2 \sin^2\beta\right) + \kappa^2(\lambda - 1)}\left[P_0\left(\frac{\kappa^2 + r_i^2 \sin^2\beta}{\kappa^2}\right) - \frac{Y}{2}\right]
\end{aligned}
\tag{26}
$$

where r_i is the tunnel radius and d_i $(= \kappa\coth\alpha_i)$ is the depth of the tunnel axis from the surface. Considering the conditions of the problem, following [54] the final form of the equation giving the shape of plastic zone is given below:

$$
\left(\frac{r_c}{r_i}\frac{d_i - r_i\cos\beta}{d_c - r_c\cos\beta}\right)^{1-\lambda} = \frac{[2M_0 + \kappa^2(\lambda - 1)][Y + P_i(\lambda - 1)]}{2M_0[Y + P_0(\lambda - 1)]}
\tag{27}
$$

where $M_0 = \kappa^2 + r_c^2 \sin^2\beta$.

In **Figure 15**, a parametric study of the plastic zone shape is shown [54].

Eq. (27) can be solved, also, by using MATLAB [56]. In **Figure 16**, an example is shown.

The analytical solution of this problem apart from its theoretical interest could be used in conjunction with computational analysis in practical problems [57]. In [55] a very important case is presented where the task was for a new tunnel to
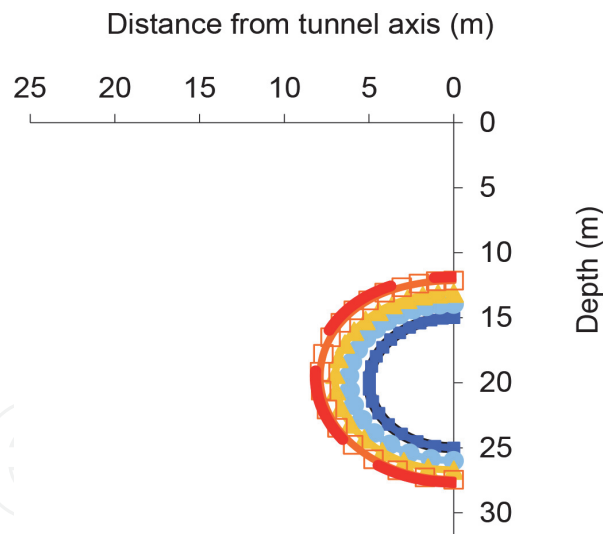

Figure 15.
Plastic zone formation for different P_i/P_o values for P_o = 500 kPa, c = 100 kPa, φ = 25°, tunnel's depth = 20 m and r = 5 m [54].
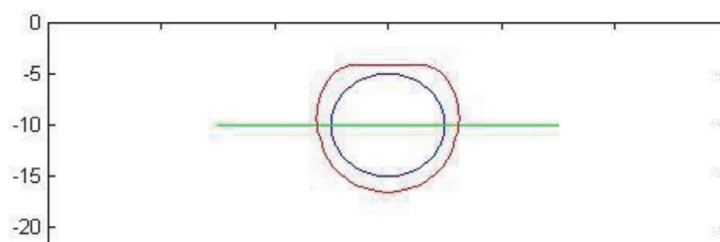

Figure 16.
Plastic zone around shallow tunnel with MATLAB. Example SMG1 [54]: D = 10 m, r = 5 m, γ = 25 kN/m³, P_o = 250 kPa, P_i = 50 kPa, c = 60 kPa, φ = 25°.

underpass the monumental Chandpole Gate in Jaipur, India. From the closed-form solution, the critical internal pressure was calculated to start with a further computational search for the optimum EPBM pressure in order to minimize the surface settlements induced by the excavation. For a more deep analysis of this problem, it seems that we have to proceed using semi-analytical methods. For the current status of this research, see [58, 59]. Important developments have been presented by Schofield [60] and Mair [61] in their Rankine Lectures of 1980 and 2008, respectively.

4. Applications of computational methods in tunnel engineering

In the last section of the chapter, a short, not complete, survey of computational methods in tunnel engineering is presented. It is a rather chronological account of methods and tools based on author's personal experience.

To start with, in **Figure 17** a very useful and clear classification of methods of analysis is presented [62–64]. For an extensive review of numerical analysis, see Potts [65].

4.1 Level 1: basic numerical methods: 1:1 mapping

The available numerical methods (FEM, BEM, DEM) belong to category "C" making "one-to-one mapping". The meaning of this term is that they make a direct modeling of geometry and physical mechanisms [63]. In the 1970s finite element method (FEM) codes, based on differential equation formulation, were developed running in mainframe computers. Towards the end of the 1970s, the boundary element method (BEM) was developed, based on integral equation formulation. Bray and his co-workers introduced a 2D indirect formulation of BEM, and they developed a code included in [13].

Based on the example presented in Hoek and Brown ([13], p. 499), a twin cavern problem was analysed using the indirect BEM formulation [66]. In order to check the numerical analysis, a photoelastic model was, also, analysed. The BEM code was modified, to plot isochromes and isoclinics [14] obtained from
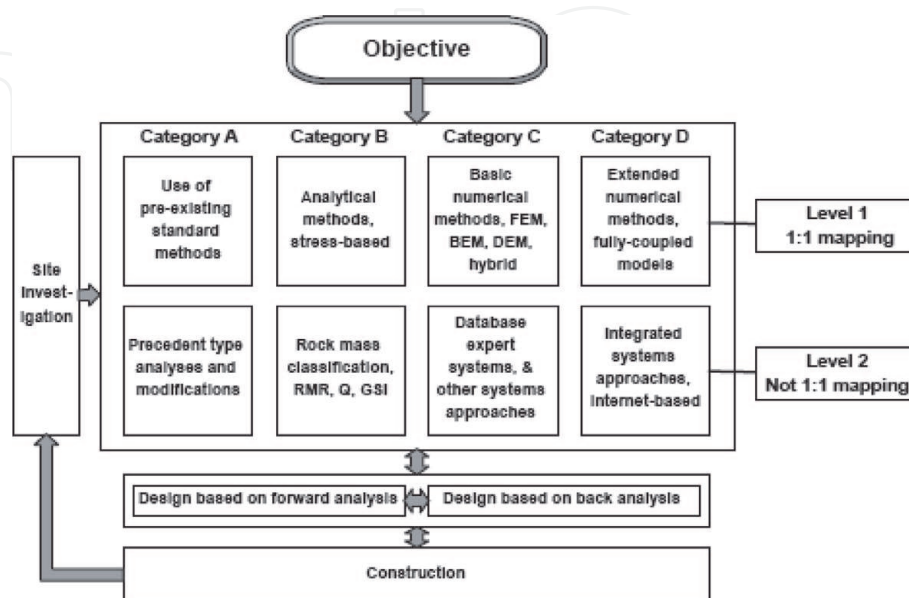

Figure 17.
The four basic methods, in two levels, comprising eight different approaches to rock mechanic modeling [62–64].

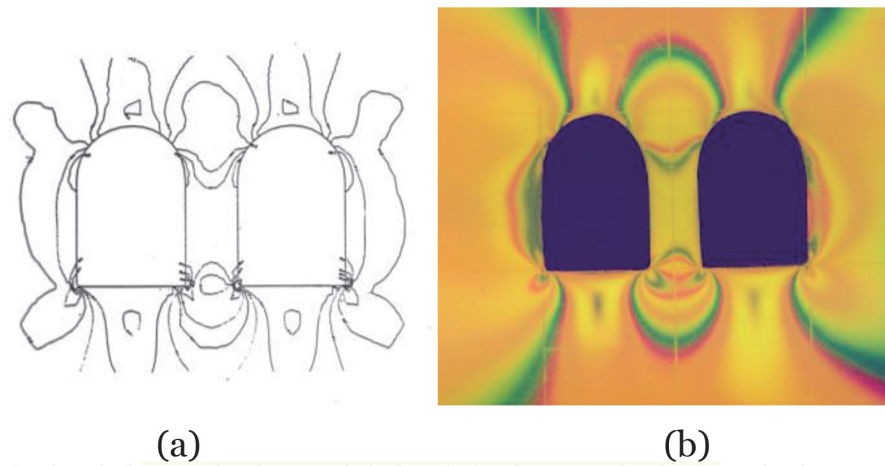(a)   (b)

Figure 18.
Plotting of isochromes of the twin cavern case. (a) Curves obtained from the numerical analysis and (b) curves obtained from the experiment [66].

photoelasticity, for comparison. In **Figure 18**, plotting of isochromes and those obtained from the experiment is shown. The agreement between the two is remarkable [66].

In a later stage (2002), with the advances in information systems and methods, the numerical methods to solve engineering problems advanced exponentially. A 3D FEM code was developed, and an extensive study was undertaken for the modeling of rock mass and underground excavations [52]. In that code several failure criteria were implemented. It may be the only 3D FEM code running the elliptic paraboloid criterion described in Section 3.1. In order to benefit from the 3D capabilities of the code, a more complicated problem was analysed. The cavern section included in [13] was modified to include, also, a tunnel of circular section cutting the cavern at a right angle (**Figures 19** and **20**). The rock mass is assumed to be anisotropic with two families of joints [51]. In formulating the problem, the following assumptions have been made: modulus of elasticity E = 7 GPa, ν = 0.25, γ = 25 kN/m^3, tunnel's depth Z = 400 m, vertical stress at infinity p = 10 MPa and in situ stress ratio k = 0.8. The model had 1441 nodes with 4323 degrees of freedom. About 236 isoparametric hexahedral elements with 20 nodes were used.

In the following figures, some characteristic results are presented. In **Figure 19**, the formation of plastic zones around the tunnels in the conjunction area is presented. Because of the anisotropy of the problem, the plastic zones are not symmetric. In **Figure 20**, the convergences of the excavation boundaries are shown.
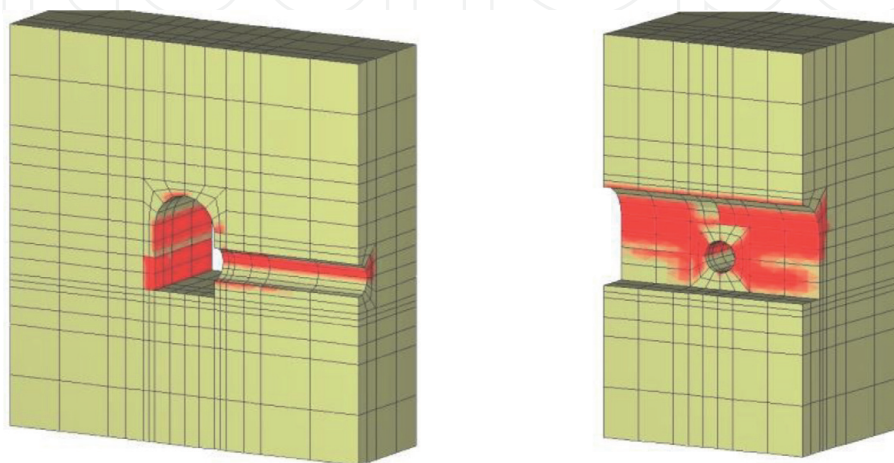

Figure 19.
Plastic zone formation around the excavations according to elliptic paraboloid failure criterion [52].
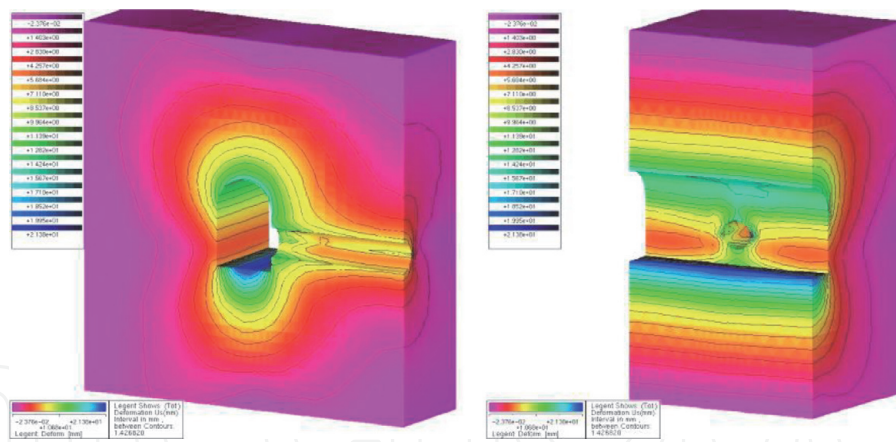
Figure 20.
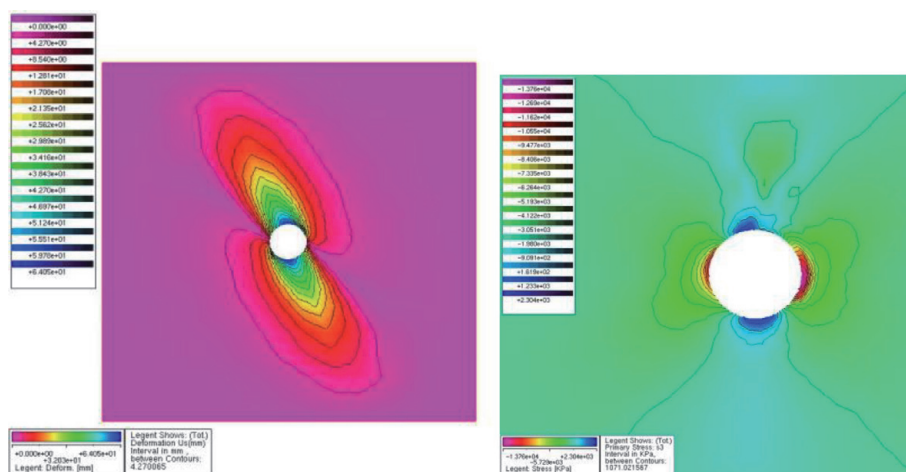*Convergences at the excavation boundaries [52].*

Figure 21.
Displacement contours (k = 0, β = 30°, r = 0.05, s = 0.013) and σ₃ stress contours (k = 0, β = 30°, r = 0.60, s = 0.91) [52].

Finally, in **Figure 21**, the displacement and stress contours are shown. The *r* and *s* coefficients are defined as *r* = *E'*/*E* and *s* = *G'*/*G*. All excavations are assumed to be unlined.

4.2 Level 2: system approaches: non-1:1 mapping

In the last paragraph of this chapter, the application of artificial intelligence (AI) methods and tools in tunnel engineering is shortly discussed. This category of methods belongs to Level 2 methods achieving a non-1:1 mapping (**Figure 17**). In this category of methods, the rock or soil mass is mapped indirectly by a network of nodes [67]. In the 1990s some applications of AI in geotechnical engineering were published [68–74]. From 2001 a great number of application of AI methods in geotechnical engineering have been published. There are two categories of approaches: the supervised learning and the unsupervised learning. Backpropagation, which was the first method applied in geotechnical engineering, belongs to the first category. Interconnected nodes corresponding to parameters involved in the problem represent the physical problem. The output of the training process is taken as a known target [67]. On the contrary, in unsupervised learning methods, the system has to extract knowledge from the data resulting in the under-lying interconnections of the parameters of the problem [75]. Currently, a great number of publications are available using more advanced and sophisticated AI

methods. A critical factor is the quality of data and the engineering judgment of the users. There are cases where the overtraining of the system resulted in a "blind" learning of the data guiding to wrong conclusions. The ability to "include creative ability, perception and judgment" [67] is, still, not achieved.

Here, an attempt to train a backpropagation network system using surface settlements induced by underground excavations is presented [76]. The total amount of the available data is 90 records, coming from different types of ground profiles and referring to tunnels constructed with different methods of excavation [77]. The provided information includes tunnel size and depth (Zo), maximum settlement (w), settlement trough width (i), volume (Vs), ground description, geological properties and method of working. An indicative part of the available data is given in **Table 4**.

The range of values of the data, the type of geological profiles and the excavated methods are given in **Table 5** [77].

In training the ANN, two approaches followed. In the first approach, all the available data were included. The tunnel depth and diameter have been used as input data and the surface settlement as output. Qualitative "data" as the geological conditions and the excavation method were not initially taken into consideration as parts of the training process. The training was not successful because we mixed the nonhomogeneous data. Therefore we proceeded to the second approach using all available data and information. To this end, we assigned a number to distinct different geological conditions and excavation method. In this training four inputs were used and the training was successful. In **Figure 22**, the relative importance of the parameters involved to the problem is shown. From this figure, we may conclude that the geometry of the tunnel, i.e. radius and depth, is the main factor with geological profile and excavation method having an important contribution too [76].

Tunnel	Tunnel data		Maximum recorded settlement	Ground geotechnical properties		Volumes	Settlement trough width	Tunneling method and soil conditions
	Depth z_o (m)	2R (m)	w (mm)	c_u (kN/m^2)	$\gamma z_o/ c_u$	V_s (%)	i (m)	
London transport fleet line green park	29.30	4.15	6.17	270	2.1	1.40	12.6	Shield construction Stiff, fissured overconsolidated London clay
NWA sewerage scheme, Hebburn	7.50	2.01	7.86	75	2.0	2.42	3.9	Shield construction Laminated clay overlain by stony clay
NWA sewerage scheme, Willington Quay Syphon, Contract 32	13.37	4.25	81.50	33	9.4	13.10	9.1	Shield construction Silty

Case history data on some tunnels and tunneling conditions [76, 77].

Table 4.
Indicative examples of case history data [76, 77].

	zo (m)	2R (m)	w (mm)
Min	3.40	1.26	1.50
Max	37.49	30.50	280.00
Geology	Homogeneous formations		
	Heterogeneous formations		
Excavation method	Shield construction		
	Hand excavation		
	Slurry shield		
	Shieldless excavation		
	Full face tunneling machine		
	Hydro-shield		
	Full face blasting		

Table 5.
Range of values of the available data and the categories of geological profiles and excavation methods [76, 77].
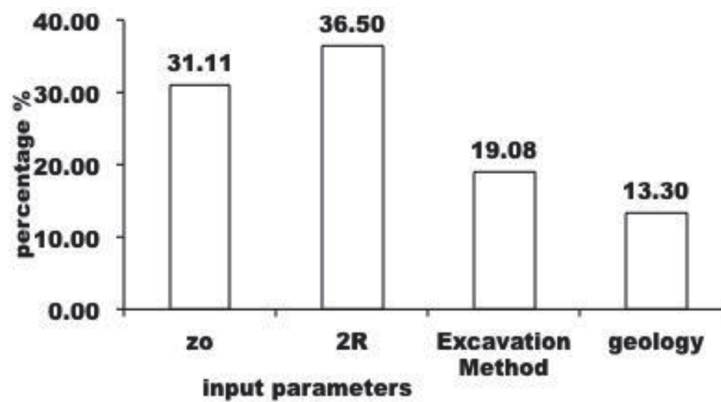

Figure 22.
Relative importance of the parameters contributing to induced settlements due to tunneling [76].

Further tunneling applications using AI tools can be found in the literature. In Zaré and Lavasan [78] an objective system approach is adopted to quantify the interaction of parameters involved in the problem of tunnel face stability. The method is based on a backpropagation ANN approach. A different approach of objective system approach, which adopted the unsupervised type of learning based on self-organizing maps, is, also, published with applications in rock engineering problems [75, 79–85].

5. Conclusions

In this chapter, a rather subjective view of tunnel engineering is presented. Nevertheless, the progress made in analytical and computational methods was followed with an effort to be well documented. Starting from a well-known problem of the elastic stress field around a circular deep tunnel, we investigated the influence of tunnel's shape in stress and displacement fields around a tunnel of the horseshoe section, as well as the extent of the influence zone for several stress fields. To this end Muskhelishvili's complex variable formulations of stress functions were

used. The next problem was the case of the shallow circular tunnel for which established elastic solutions are presented. Proceeding to the more difficult problem of the plastic analysis, we examined the case of deep tunnels, and then we presented a closed-form solution of the plastic zone formation for the shallow circular tunnel. This is a topic still needing further investigation because of its mathematical difficulty. Computational methods were the last part of the chapter. A classification of methods was presented followed by a problem of deep tunnels analyzed using 3D finite element analysis. The increasing exploitation of artificial intelligence tools in analyzing geotechnical problems was the last topic. The presentation was based on the tunneling-induced surface settlements as a paradigm. The cited references listed below are a basic and indicative selection of literature for further reading.

Acknowledgements

Author details

Michael G. Sakellariou
National Technical University of Athens, Athens, Greece

*Address all correspondence to: mgsakel@mail.ntua.gr

IntechOpen

References

[1] Diamond RS, Kassel BG. A history of the urban underground tunnel (4000 B. C.E.–1900 C.E.). Journal of Transportation Technologies. 2018;**8**: 11-43. DOI: 10.4236/jtts.2018.81002

[2] Dani AH, Mohen J-P, editors. UNESCO History of Humanity Volume II, From the Third Millennium to the Seventh Century BC. New York: Routledge Reference, Chapman and Hall; 1996. 624 p. ISBN: 0-415-09306-6

[3] Széchy K. The Art of Tunnelling. 2nd ed. Budapest: Akadémiai Kiadó; 1973. 1097 p

[4] Frumkin A, Shimron A. Tunnel engineering in the iron age: Geoarchaeology of the Siloam Tunnel, Jerusalem. Journal of Archaeological Science. 2006;**33**:227-237. DOI: 10.1016/j.jas.2005.07.018

[5] Apostol T. The tunnel of Samos. Engineering & Science. 2004;**1**:30-40. ISSN: 0013-7812

[6] Mainland East Division, Catalogue of Notable Tunnel Failures—Case Histories (up to April 2015). Prepared by Mainland East Division Geotechnical Engineering Office, Civil Engineering and Development Department (CEDD). The Government of the Hong Kong Special Administration Region; 2005. 350 p

[7] Bieniawski ZT. Geomechanics classification of rock masses and its application in tunnelling. In: Proceedings of the Third International Congress on Rock Mechanics, ISRM; Denver. Vol IIA. 1974. pp. 27-32

[8] Bieniawski ZT. Rock Mechanics Design in Mining and Tunnelling. Rotterdam: A.A. Balkema; 1984. 272 p

[9] Barton N. Recent experience with the Q-system of tunnel support design. In: Bieniawski ZT, editor. Proceedings Symposium Exploration for Rock Engineering. Vol. 1. 1976. pp. 10-114

[10] Timoshenko SP, Goodier JN. Theory of Elasticity. New York: McGraw-Hill; 1970. 576 p

[11] Terzaghi K. Theoretical Soil Mechanics. New York: John Wiley; 1943. 510 p

[12] Jaeger JC, Cook NGW, Zimmerman RW. Fundamentals of Rock Mechanics. 4th ed. Malden, Oxford, Victoria: Blackwell Publishing; 2007. 475 p

[13] Hoek E, Brown ET. Underground Excavations in Rock. London: The Institution of Mining and Metallurgy; 1980. 527 p. ISBN: 0 900488 55 7

[14] Frocht MM. Photoelasticity. Vol. 1 & 2. New York: John Wiley & Sons; 1941. 411 p. & 505 p

[15] Theocaris PS, Koroneos E. Stress distribution around a tunnel situated in a layer under the action of gravity. Rock Mechanics. 1972;**4**:139-154. DOI: 10.1007/BF01596999

[16] Theocaris PS. Moiré Fringes in Strain Analysis. Oxford: Pergamon Press; 1969. 426 p

[17] Zienkiewicz OC. The Finite Element Method in Engineering Science. 2nd ed. London: McGraw-Hill; 1971. 521 p

[18] Crouch SL, Starfield AM. Boundary Elements Methods in Solid Mechanics. 2nd ed. London: Allen & Unwin; 1974. 322 p

[19] Cundall PA, Strack ODL. Discrete numerical model for granular assemblies. Geotechnique. 1979;**29**(1): 47-65. DOI: 10.1680/geot.1979.29.1.47

[20] Liu GR. Meshfree Methods: Moving Beyond the Finite Element Method. 2nd ed. USA: CRC Press; 2018. 792 p

[21] Fern J, Rohe A, Soga K, Alonso E. Material Point Method for Geotechnical Engineering: A Practical Guide. CRC Press, Francis Taylor Group; 2019. 420 p

[22] Gudehus G, editor. Finite Elements in Geomechanics. London: John Wiley; 1977. 573 p

[23] Desai CS, Christian JT, editors. Numerical Methods in Geotechnical Engineering. New York: McGraw-Hill; 1977. 783 p

[24] Jeffery MA. Plane stress and plain strain in bipolar co-ordinates. Philosophical Transactions of the Royal Society of London. Series A. 1920: 265-293

[25] Gerçek H. The past revisited: The giants behind the elastic solutions for stresses around underground openings. In: Ulusay R, Aydan O, Gerçek H, Ali Hindistan M, Tuncay E, editors. Rock Mechanics & Rock Engineering: From the Past to the Future, Vol. 1. CRC Press; 2016. pp. 409-414

[26] Schürch R, Anagnostou G. The applicability of the ground response curve to tunnelling problems that violate rotational symmetry. Rock Mechanics and Rock Engineering. 2012; **45**:1-10. DOI: 10.1007/s00603-011-0182-1

[27] Muskhelishvili N. Some Basic Problems of the Mathematical Theory of Elasticity. Groningen, The Netherlands: P. Noordhoff, Ltd.; 1963. xxx p

[28] Gerçek H. An elastic solution for stresses around tunnels with conventional shapes. International Journal of Rock Mechanics & Mining Sciences. 1997;**34**(3–4):96.e1-96.e14. DOI: 10.1016/S1365-1609(97)00091-9

[29] Angelopoulou O. Calculation of stresses, strains and displacements around a Horseshoe tunnel section with conformal mapping; Application in k=0 and k=1/3 stress fields [M.Eng. thesis]. Athens: National Technical University of Athens (in Greek); 2004

[30] Karanasiou S. Calculation of stresses, strains and displacements around a Horseshoe tunnel section with conformal mapping; Application in k=1 and k=3 stress fields [M.Eng. thesis]. Athens: National Technical University of Athens (in Greek); 2004

[31] Bray JW. Some applications of elastic theory. In: Brown ET, editor. Analytical and Computational Methods in Engineering Rock Mechanics. London: Allen & Unwin; 1987. pp. 32-94

[32] Savin GN. Stress Concentration Around Holes. In: Gros E, editor (trans.) Oxford: Pergamon; 1961. 997 p

[33] Tzoumas A. Study of the influence of surface boundary on the stress field around circular and horseshoe tunnel sections. Linear and non-linear approach of rock behaviour [M.Sc. thesis]. Athens: National Technical University of Athens; 2006

[34] Mindlin RD. Stress distribution around a tunnel. Transactions of American Society of Civile Engineers. 1940;**105**:1117-1153

[35] Poulos HG, Davies EH. Elastic Solutions for Soil and Rock Mechanics. J. Wiley & Sons; 1974. 411 p

[36] Malvern LE. Introduction to the Mechanics of a Continuous Medium. New Jersey: Prentice Hall; 1969. 713 p

[37] Strack OE. Analytic solutions of elastic tunnelling problems [PhD thesis]. Delft: Delft University; 2002

[38] Verruijt A. Deformations of an elastic half space with a circular cavity.

International Journal of Solids and Structures. 1998;**35**(21):2795-2804. DOI: 10.1016/S0020-7683(97)00194-7

[39] Verruijt A, Booker JR. Surface settlements due to deformation of a tunnel in an elastic half plane. Géotechnique. 1996;**46**(4): 753-756. DOI: 10.1680/geot.1998.48. 5.709

[40] Pelli E, Sofianos A. Analytical calculation of the half space stress field around tunnels under seismic loading of SW waves. Tunnelling and Underground Space Technology. 2018; **79**:150-174. DOI: 10.1016/j. tust.2018.01.019

[41] Sokolovskii VV. Statics of Soil Media. London: Butterworths S.P; 1960. 237 p

[42] Hill R. The Mathematical Theory of Plasticity. 2nd ed. London: Oxford University Press; 1998. 372 p

[43] Chen WF. Limit Analysis and Soil Plasticity. Amsterdam: Elsevier Scientific Publishing Company; 1975. 638 p

[44] Davis RO, Selvadurai APS. Plasticity and Geomechanics. Cambridge: Cambridge University Press; 2002. 287 p

[45] Schofield A, Wroth P. Critical State Soil Mechanics. London: McGraw-Hill; 1968. 310 p

[46] Yu MH. Advances in strength theories for materials under complex stress state in the 20th century. Applied Mechanics Reviews. 2002;**55**:169-218. DOI: 10.1115/1.1472455

[47] Vrakas A, Anagnostou G. A simple equation for obtaining finite strain solutions from small strain analyses of tunnels, with very large convergences. Géotechnique. 2015;**65**(11):936-944. DOI: 10.1680/jgeot.15.P.036

[48] Kachanov LM. Foundations of the Theory of Plasticity. Amsterdam: North Holland Publishing Company; 1971. 482 p

[49] Detourney E, St. John M. Design charts for a deep circular tunnel under non-uniform loading. Rock Mechanics and Rock Engineering. 1988;**21**:119-137. DOI: 10.1007/BF01043117

[50] Theocaris PS. Failure criteria for isotropic bodies revisited. Engineering Fracture Mechanics. 1995;**51**:239-264. DOI: 10.1016/0013-7944(94)00270-R

[51] Theocaris PS. Failure loci of some igneous and metamorphic rocks. Rock Mechanics and Rock Engineering. 1999; **32**(4):267-290. DOI: 10.1007/ s006030050048

[52] Kozanis S. Towards the study of the rock-mass, considered as a medium with non-linear-anisotropic behaviour, using finite element methods. With emphasis on underground structures [PhD thesis]. Athens: National Technical University of Athens; 2002 (in Greek)

[53] Apostoleris K. Investigation of plastic zone formation around a circular tunnel in isotropic stress field by applying the elliptic paravoloid criterion [MSc thesis]. Athens: National Technical University of Athens; 2003 (in Greek)

[54] Massinas S, Sakellariou M. Closed form solution for plastic zone formation around a circular tunnel in half space obeying Mohr-Coulomb criterion. Géotechnique. 2009;**59**(8):691-701. DOI: 10.1680/geot.8.069

[55] Massinas S, Prountzopoulos G, Bhardwaj V, Saxena A, Clark J, Sakellariou M. Design aspects of under-passing a city's heritage landmark with EPB machines under low overburden: The case of Chandpole Gate in Jaipur Metro, India. Geotechnical & Geological

Engineering. 2018;**36**(6):3683-3705. DOI: 10.1007/s10706-018-0565-0

[56] Fragouli G. Numerical solution of the plastic zone formation around shallow circular tunnels [MEng thesis]. Athens: National Technical University of Athens; 2010 (in Greek)

[57] Massinas S. Analytic solution for shallow tunnelling problems in elastic-plastic half space [PhD thesis]. Athens: National Technical University of Athens; 2020

[58] Zou JF, Wei A, Yang T. Elasto-plastic solution for schallow tunnel in semi-infinite space. Applied Mathematical Modelling. 2018;**64**: 669-687. DOI: 10.1016/j. apm.2018.07.049

[59] Zou JF, Wang F, Wei A. A semi-analytical solution for shallow tunnels with radius-iterative-approach in semi-infinite space. Applied Mathematical Modelling. 2019;**73**: 285-302. DOI: 10.1016/j.apm.2019. 04.007

[60] Schofield AN. Cambridge geotechnical centrifuge operations. Géotechnique. 1980;**30**(3):227-268. DOI: 10.1680/geot.1980.30.3.227

[61] Mair R. Tunnelling and geotechnics: New horizons. Géotechnique. 2008; **58**(9):695-736. DOI: 10.1680/ geot.2008.58.9.695

[62] Hudson JA. Rock engineering case histories: Key factors, mechanisms and problems. In: Elorante P, Sarkka P, editors. Rock Mechanics—A Challenge for Society. Rotterdam: Balkema; 2001. pp. 13-20

[63] Jing L, Hudson JA. Numerical methods in rock mechanics. International Journal of Rock Mechanics and Mining Sciences. 2002;**39**: 409-427. DOI: 10.1016/S1365-1609(02) 00065-5

[64] Jing L. A review of techniques, advances and outstanding issues in numerical modelling for rock mechanics and rock engineering. International Journal of Rock Mechanics and Mining Sciences. 2003;**40**:283-353. DOI: 10.1016/S1365-1609(03)00013-3

[65] Potts D. Numerical analysis: A virtual dream or practical reality? Géotechnique. 2003;**53**(6):535-573. DOI: geot.2003.53.6.535

[66] Sklavounos P. Experimental and numerical modelling of underground excavations in rock: Application in horseshoe sections [MEng thesis]. Athens: National Technical University; 1986 (in Greek)

[67] Sakellariou M, Ferentinou M. A study of slope stability prediction using neural networks. Geotechnical and Geological Engineering. 2005;**23**: 419-445. DOI: 10.1007/s10706-004-8680-5

[68] Millar DL, Hudson JA. Performance monitoring of rock engineering systems utilising neural networks. Transactions of Institute of Mining and Metallurgy, Section A. 1996;**103**:A13-A16

[69] Goh ATC. Seismic liquefaction potential assessed by neural networks. Journal of Geotechnical Engineering. 1995;**120**(9):1467-1480. DOI: 10.1061/ (ASCE)0733-9410(1994)120:9(1467)

[70] Goh ATC. Back-propagation neural networks for modelling complex systems. Artificial Intelligence Engineering. 1995;**9**:143-151. DOI: 10.1016/0954-1810(94)00011-S

[71] Sklavounos P, Sakellariou M. Rock mass classification. In: Proceedings of the 10th International Conference on Applications of Artificial Intelligence in Engineering. July 1995 Udine; Computational Mechanics Publications. 1995. pp. 269-276. DOI: 10.2495/ AI950411

[72] Najjar YM, Basheer IA. Utilising computational neural networks for evaluating the permeability of compacted clay liners. Geotechnical and Geological Engineering. 1996;**14**: 193-212. DOI: 10.1007/BF00452947

[73] Gangopadhyay S, Gautam TR, Das Gupta A. Subsurface characterisation using artificial neural network and GIS. Journal of Computers in Civil Engineering. 1999;**13**:153-161. DOI: 10.1061/(ASCE)0887-3801(1999)13:3 (153)

[74] Roussos E. Neural networks for landslide hazard estimation [MSc thesis]. London: King's College; 2000

[75] Ferentinou M, Sakellariou M. Computational intelligence tools for the prediction of slope performance. Computers and Geotechnics. 2007;**34**: 362-384. DOI: 10.1016/j.compgeo.2007. 06.004

[76] Kapsampeli A. Application of neural networks in the study of surface settlements induced by excavation of tunnels in urban environment [MEng thesis]. Athens: National Technical University of Athens; 2007 (in Greek)

[77] Attewell PB, Yeates J, Selby AR. Soil Movements Induced by Tunnelling and their Effects on Pipelines and Structures. New York: Blackie; 1986. 325 p

[78] Zaré M, Lavasan AA. A new face vulnerability index for mechanized tunnelling in subsoil. In: Peila Viggiani C, editor. Tunnels and Underground Cities: Engineering and Innovation meet Archaeology, Architecture and Art. London: Taylor & Francis Group; 2019. pp. 1225-1233. ISBN: 978-1-138-38865-9

[79] Ferentinou M. Evaluation of landslides risk using artificial neural networks in a GIS environment [PhD thesis]. Athens: National Technical University of Athens; 2004 (in Greek)

[80] Ferentinou M. Sakellariou M. Assessing landslide hazard on medium and large scales, using self-organising maps. In: Hungr O, Fell R, Couture R, Eberhardt E, editors. Landslide Risk Management. Joint 2005 International Conference on Landslide Risk Management/18th Annual Vancouver Geotechnical Society Symposium; Vancouver; Taylor & Francis; 2005. pp. 639-648. eBook ISBN: 9780429151354

[81] Ferentinou M, Hasiotis T, Sakellariou M. Clustering of geotechnical properties of marine sediments through self-organizing maps —An example from the Zakynthos Canyon-Valley system, Greece. In: Mosher DC et al., editors. Submarine Mass Movements and Their Consequences, Advances in Natural and Technological Hazards Research. Vol. 28. Springer Science + Business Media B.V.; 2010. pp. 43-54. Online ISBN: 978–90–481-3071-9

[82] Ferentinou M, Karymbalis E, Charou E, Sakellariou M. Using self organizing maps in applied geomorphology. In: Mwasiagi JI, editor. Self Organizing Maps—Applications and Novel Algorithm Design. InTech Publisher; 2011. pp. 273-298. DOI: 10.5772/13265. Chapter 15. 978-953-307-546-4

[83] Ferentinou M, Hasiotis T, Sakellariou M. Application of computational intelligence tools for the analysis of marine geotechnical properties in the head of Zakynthos canyon, Greece. Computers & Geosciences. 2012;**40**:166-174. DOI: 10.1016/j.compgeo.2007.06.004

[84] Matziaris V, Ferentinou M, Sakellariou M. Elaboration of a high-dimensional database of unsaturated soils using artificial neural networks.

In: 2nd European Conference on
Unsatuturated Soils E-UNSAT 2012,
Unsaturated Soils, Research and
Applications, Napoli, Italy. 2012. 457 p.
Online ISBN: 978–3–642-31343-1

[85] Ferentinou M, Sakellariou M.
Introduction of an objective matrix
coding method for rock engineering
systems through self organising maps.
In: Proceedings of the 13th International
Congress of Rock Mechanics (ISRM);
10–13 May 2015; Montreal. ISRM-13
CONGRESS-2015-374